



UvA-DARE (Digital Academic Repository)

Two Point functions in 4-d Dynamical Triangulation

de Bakker, B.V.; Smit, J.

Published in:
Nuclear Physics B

DOI:
[10.1016/0550-3213\(95\)00381-2](https://doi.org/10.1016/0550-3213(95)00381-2)

[Link to publication](#)

Citation for published version (APA):
de Bakker, B. V., & Smit, J. (1995). Two Point functions in 4-d Dynamical Triangulation. Nuclear Physics B, 454(B), 343-356. [https://doi.org/10.1016/0550-3213\(95\)00381-2](https://doi.org/10.1016/0550-3213(95)00381-2)

General rights

It is not permitted to download or to forward/distribute the text or part of it without the consent of the author(s) and/or copyright holder(s), other than for strictly personal, individual use, unless the work is under an open content license (like Creative Commons).

Disclaimer/Complaints regulations

If you believe that digital publication of certain material infringes any of your rights or (privacy) interests, please let the Library know, stating your reasons. In case of a legitimate complaint, the Library will make the material inaccessible and/or remove it from the website. Please Ask the Library: <https://uba.uva.nl/en/contact>, or a letter to: Library of the University of Amsterdam, Secretariat, Singel 425, 1012 WP Amsterdam, The Netherlands. You will be contacted as soon as possible.



ELSEVIER

Nuclear Physics B 454 (1995) 343-354

NUCLEAR
PHYSICS B

Two-point functions in 4D dynamical triangulation

Bas V. de Bakker¹, Jan Smit²

*Institute for Theoretical Physics, University of Amsterdam, Valckenierstraat 65, 1018 XE Amsterdam,
The Netherlands*

Received 8 March 1995; revised 10 July 1995; accepted 17 July 1995

Abstract

In the dynamical triangulation model of 4D Euclidean quantum gravity we measure two-point functions of the scalar curvature as a function of the geodesic distance. To get the correlations it turns out that we need to subtract a squared one-point function which, although this seems paradoxical, depends on the distance. At the transition and in the elongated phase we observe a power law behaviour, while in the crumpled phase we cannot find a simple function to describe it.

1. Introduction

In the dynamical triangulation model of four-dimensional Euclidean quantum gravity the path integral over metrics on a certain manifold is defined by a weighted sum over all ways to glue four-simplices together at the faces [1,2]. This idea was first formulated in [3], using hypercubes instead of simplices.

The partition function of the model at some fixed volume N is

$$Z(N, \kappa_2) = \sum_{T(N_4=N)} \exp(\kappa_2 N_2). \quad (1)$$

The sum is over all ways to glue N four-simplices together, such that the resulting complex has some fixed topology which is usually (as well as in this article) taken to be S^4 . The N_i are the number of i -simplices in this complex. κ_2 is a coupling constant, which is proportional to the inverse of the bare Newton constant: $\kappa_2 \propto G_0^{-1}$.

¹ E-mail: bas@phys.uva.nl.

² E-mail: jsmit@phys.uva.nl.

It turns out that the model has two phases. For low κ_2 the system is in a crumpled phase, where the average number of simplices around a vertex is large and the average distance between two simplices is small. In this phase the volume within a distance r appears to increase exponentially with r , a behaviour like that of a space with constant negative curvature. At high κ_2 the system is in an elongated phase and resembles a branched polymer. As is the case with a branched polymer, the (large scale) internal fractal dimension is 2. The transition between the two phases occurs at a critical value κ_2^c which depends somewhat on N . This transition appears to be a continuous one, making a continuum limit possible [4–6]. At the transition, the space behaves in several respects like the four-dimensional sphere [7].

2. Curvature and volume

In the Regge discretization of general relativity, all the simplices are pieces of flat space. The curvature is concentrated on the subsimplices of codimension two, in our case the triangles. On these triangles it is proportional to a two-dimensional delta function. From the definition of curvature as the rotation of a parallel transported vector, one can find the integrated curvature over a small region $V_\epsilon(\Delta)$ around such a triangle

$$\int_{V_\epsilon(\Delta)} R\sqrt{g} dx = 2A_\Delta \delta_\Delta, \quad (2)$$

where A_Δ is the area of the triangle and δ_Δ is the deficit angle around the triangle (see e.g. Ref. [8]). The deficit angle around a triangle is the angle which is missing from 2π

$$\delta_\Delta = 2\pi - \sum_{d \in \{S(\Delta)\}} \theta_d, \quad (3)$$

where $\{S(\Delta)\}$ are the simplices around the triangle and θ_d is the angle between those two faces of the simplex that border the triangle. The angle δ_Δ can be negative.

In dynamical triangulation, all the simplices have the same size and shape and the deficit angle is a simple function of the number n_Δ of simplices around the triangle. Then expression (2) reduces to

$$\int_{V_\epsilon(\Delta)} R\sqrt{g} dx = 2V_2(2\pi - \theta n_\Delta), \quad (4)$$

where θ is the angle between two faces of a simplex, which for D dimensions equals $\arccos(1/D)$, and $V_2 = A_\Delta$ is the now constant area of a two-simplex.

For each triangle we can define a local four-volume that belongs to the triangle by assigning that part of each adjoining simplex to it which is closer to the triangle than to any other. For equal simplices, this just results in $V_4/10$ per adjoining simplex with V_4 the volume of a four-simplex. In other words, this local volume is

$$V_{\Delta} = \int_{\Omega(\Delta)} \sqrt{g} dx = \frac{V_4}{10} n_{\Delta}, \tag{5}$$

where $\Omega(\Delta)$ is the region of space associated to that triangle. It is not clear what V_{Δ} would mean in the continuum limit. We define it here mainly to compare our results with other work on simplicial quantum gravity.

If we view the delta function curvature as the average of a constant curvature over the region $\Omega(\Delta)$, this constant curvature would be equal to

$$R_{\Delta} = \frac{20V_2}{V_4} \frac{2\pi - \theta n_{\Delta}}{n_{\Delta}}. \tag{6}$$

Because neither a constant term nor a constant factor is important for the behaviour of correlation functions, we will in the rest of this paper for convenience use the definitions

$$R_{\Delta} \equiv n_{\Delta}^{-1}, \tag{7}$$

$$V_{\Delta} \equiv n_{\Delta}. \tag{8}$$

3. Two-point functions

One of the interesting aspects of the dynamical triangulation model one can investigate is the behaviour of two-point functions of local observables. Because we are looking at observables defined on the triangles we consider correlations between the triangles, at a fixed distance d which is also defined in terms of triangles. Such a correlation function of an observable $O(x)$ will be denoted by $\langle OO \rangle(d)$.

We define the geodesic distance between two triangles as the smallest number of steps between neighbouring triangles needed to get from one to the other. For this purpose, we define two triangles to be neighbours if they are subsimplices of the same four-simplex and share an edge. Other definitions of neighbour are conceivable. One such definition would be to define two triangles to be neighbours if they share an edge, irrespective of whether they are in the same simplex. The one we use has the advantage that it is quite narrow and therefore results in larger distances.

The idea behind our correlation functions is as follows. For each configuration generated according to the ensemble (1), we take a random pair (x, y) of triangles at distance d , where x and y denote the triangles. For this pair we calculate the observable $O(x)O(y)$. Then we go to the next configuration and repeat the process. Finally we take the average over all such pairs. If no such pair exists for a particular configuration, the configuration is discarded.

Obviously, this method would be very inefficient in practice. We improve the statistics by using the average value of $O(x)O(y)$ over all pairs (x, y) at distance d in each configuration. Therefore, we calculate for each configuration

$$\frac{\sum_{x,y} O(x)O(y)\delta_{d(x,y),d}}{\sum_{x,y} \delta_{d(x,y),d}}. \tag{9}$$

Taking the average over configurations

$$\langle A \rangle = \frac{\sum_{\mathcal{T}} A \exp(\kappa_2 N_2(\mathcal{T}))}{\sum_{\mathcal{T}} \exp(\kappa_2 N_2(\mathcal{T}))}, \quad (10)$$

results in the correlation function

$$\langle OO \rangle(d) = \left\langle \frac{\sum_{x,y} O(x)O(y)\delta_{d(x,y),d}}{\sum_{x,y} \delta_{d(x,y),d}} \right\rangle. \quad (11)$$

Other definitions are conceivable. One can take random pairs of triangles from the collection of all configurations. Configurations with relatively many pairs of triangles at distance d will then be counted more often. In formula, it results in the correlation function

$$\langle OO \rangle'(d) = \frac{\left\langle \sum_{x,y} O(x)O(y)\delta_{d(x,y),d} \right\rangle}{\left\langle \sum_{x,y} \delta_{d(x,y),d} \right\rangle}. \quad (12)$$

A few experiments did not show a qualitative difference in the behaviour of (11) and (12) at the distances considered below. However, for large distances where the finite size of the configurations comes into play, the difference becomes significant.

A third possibility, which is natural in Regge calculus, treats n_x as a local volume element at x in a discrete approximation to a continuum integral over Euclidean space-time:

$$\langle OO \rangle''(d) = \frac{\left\langle \sum_{x,y} n_x n_y O(x)O(y)\delta_{d(x,y),d} \right\rangle}{\left\langle \sum_{x,y} n_x n_y \delta_{d(x,y),d} \right\rangle}. \quad (13)$$

In this paper we explore the form (11). We expect that the correlations constructed from either (11), (12) or (13) will behave identically for not too large distances. In a large system, compared to the distance under consideration, the sum over the triangles will introduce a self-averaging which probably makes the difference in averaging between (11) and (12) irrelevant.

In Fig. 1 we have plotted the correlation function of the curvature, with the square of its expectation value subtracted. Most of the data in this paper are for a volume $N = 16\,000$ simplices. The values of κ_2 correspond to a system in the crumpled phase ($\kappa_2 = 0.8$), near (but slightly below) the transition ($\kappa_2 = 1.22$) and in the elongated phase ($\kappa_2 = 1.5$).

Configurations were recorded every 10 000 sweeps, where a sweep is defined as a number of accepted moves equal to the number of simplices N . For $\kappa_2 = 0.8$, 1.22 and 1.5 we used 16, 51 and 21 configurations, respectively.

One thing is immediately striking: the correlation functions do not go to zero at long distances. To keep the short distance behaviour visible, the full range in the elongated phase has not been plotted, but we already see that also in this phase it crosses the zero axis and indeed this curve does eventually go to large (≈ 0.02) positive values.

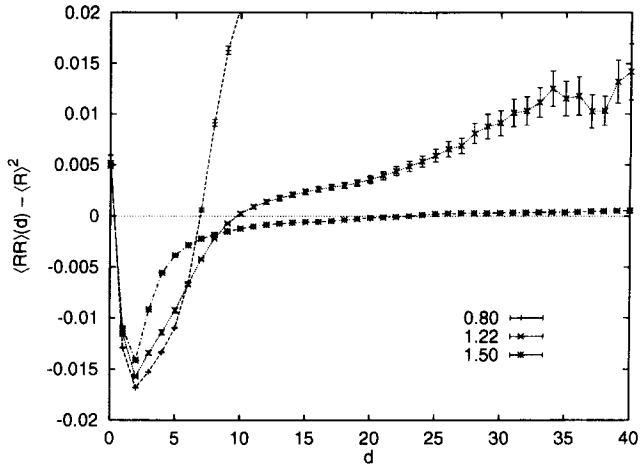


Fig. 1. The correlation function $\langle RR \rangle(d) - \langle R \rangle^2$ for various values of κ_2 .

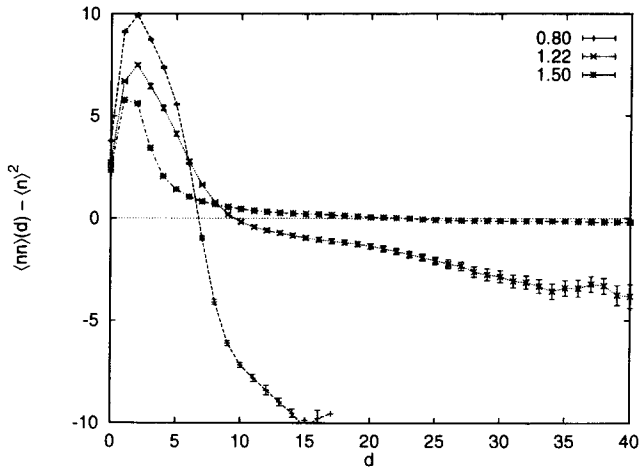


Fig. 2. The correlation function $\langle nn \rangle(d) - \langle n \rangle^2$ for various values of κ_2 .

The local volume V_Δ is proportional to the number of simplices n_i around a triangle i . We see that in this model, this observable V_Δ is essentially the same as the scalar curvature. At first sight, one would therefore expect them to have the same behaviour. If one is positively correlated, the other one would also be positively correlated. Fig. 2 shows the correlation of n . We see that quite the opposite is true. With few exceptions, n is positively correlated where $R = n^{-1}$ is negatively correlated and vice versa.

This behaviour is similar to that reported for the Regge calculus formulation of simplicial quantum gravity in Ref. [9]. There it is also found that the curvature correlations are positive and the volume correlations negative at large distances.

This difference in behaviour can be explained intuitively as follows. Because triangles

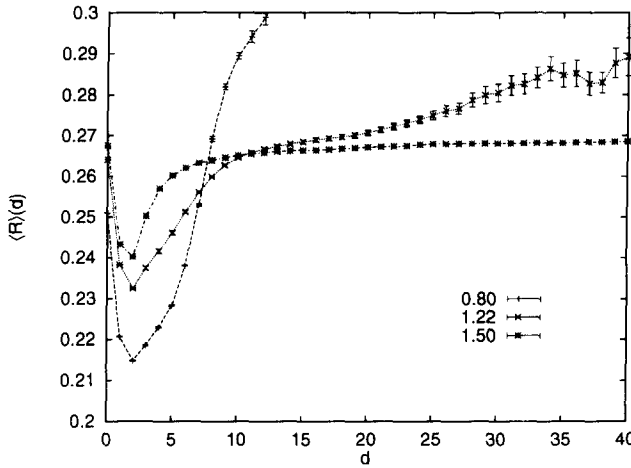


Fig. 3. The curvature as a function of the distance $\langle R \rangle(d)$ for various values of κ_2 .

with large n have more neighbours, any random triangle will have a large chance to be close to a point with large n and a small chance to be close to a point with small n . So whatever the value of n at the origin, the points nearby have large n and the points far away have small n . The average $\langle nn \rangle$ will then be large at small distances and small at large distances. Because large n means small R , the situation is reversed if we substitute R for n in this discussion, qualitatively explaining Figs. 1 and 2.

At first sight one might conclude from this explanation that a point with large n having many neighbours is just an artefact of the model. This is not true, however. Large n corresponds to large negative curvature and also in the continuum a point with large negative curvature has a larger neighbourhood. To be more precise, the volume of d -dimensional space within a radius r around a point with scalar curvature R equals

$$V(R) = C_d r^d \left(1 - \frac{R}{6(d+2)} r^2 + O(r^4) \right). \tag{14}$$

4. Connected part

The above reasoning leads us to the somewhat unusual concept of a correlation function that does not depend on some observable at the origin. We define such a correlation as

$$\langle R \rangle(d) = \left\langle \frac{\sum_{x,y} R_x \delta_{d(x,y),d}}{\sum_{x,y} \delta_{d(x,y),d}} \right\rangle, \tag{15}$$

where x and y denote a triangle. In the more usual case of a quantum field theory on flat space this could never depend on the distance, but here it does. The reason is that

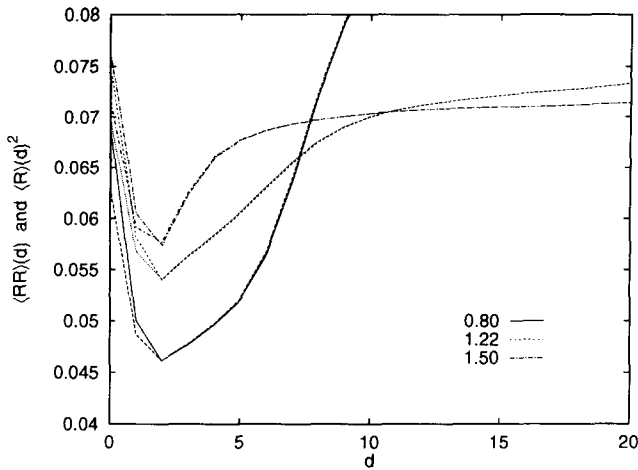


Fig. 4. Comparison between the correlation function $\langle RR \rangle(d)$ (upper curves of each pair) and the squared one-point function $\langle R \rangle(d)^2$ (lower curves) at various values of κ_2 .

we correlate functions of the geometry with the distance, which is itself a function of the geometry.

Fig. 3 shows this correlation function. No average has been subtracted. The behaviour of this one-point function turns out to be very similar to that of the curvature correlation in Fig. 1. This correlation function again shows that any particular point has a large chance to be in the neighbourhood of a point with low curvature, which can be simply explained with the fact that points with low curvature have more neighbourhood.

The same plot for n (not shown) shows the opposite behaviour. At small distances it is larger than average, while at large distances it is smaller than average. This is rather obvious, because where n is large, its inverse is small and vice versa.

We can now investigate how much of the curvature correlation shown of Fig. 1 is due to this effect. Fig. 4 compares the curvature correlation $\langle RR \rangle(d)$ with the square of this one-point function. We see that, except at small distances, the two are indistinguishable on this scale. In other words, we have not been measuring any curvature correlations. All we have measured are correlations between the curvature and the geodesic distance. Similarly, $\langle nn \rangle(d)$ and $\langle n \rangle(d)^2$ are nearly equal.

It is now easy to explain the difference in behaviour between the curvature and the volume correlations. Because they are almost equal to the square of $\langle R \rangle(d)$ and $\langle n \rangle(d)$ respectively, they behave just like them. And as we just mentioned, it is easy to understand that these have opposite behaviours.

The way to go now is to subtract the two things and see what real curvature correlations are left. This is similar to subtracting a disconnected diagram and keeping the connected part. We get the corrected correlation functions

$$C_R(d) = \langle RR \rangle(d) - \langle R \rangle(d)^2, \tag{16}$$

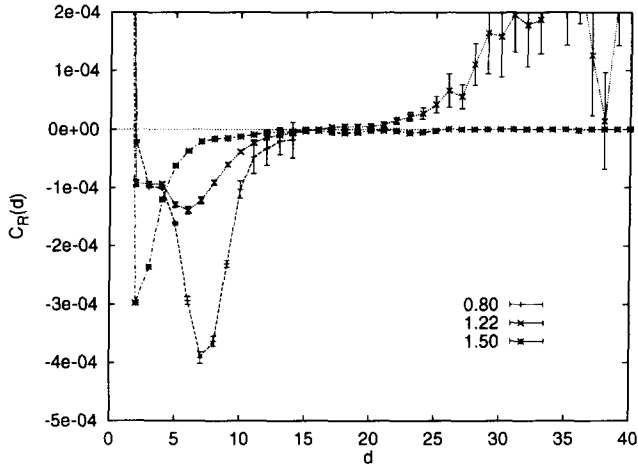


Fig. 5. Corrected correlation function $C_R(d)$ at various values of κ_2 .

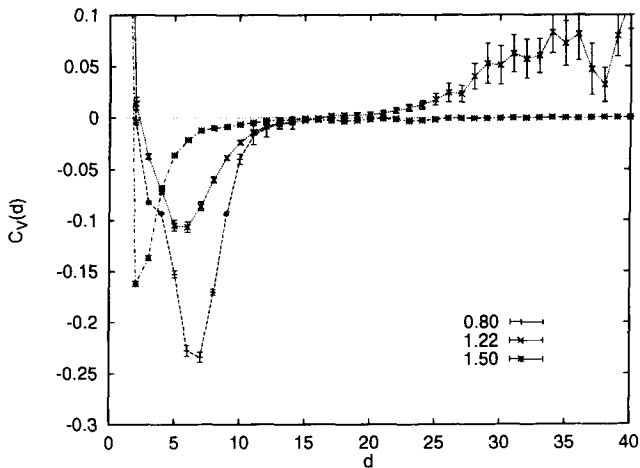


Fig. 6. Corrected correlation function $C_V(d)$ at various values of κ_2 .

$$C_V(d) = \langle nn \rangle(d) - \langle n \rangle(d)^2. \quad (17)$$

The results for the curvature are plotted in Fig. 5 and those for the volume in Fig. 6. The error bars were found by a jackknife method, each time leaving out one of the configurations in the calculation of $C_R(d)$ and $C_V(d)$. Now both correlations behave almost exactly the same. Note the large difference in scale between these figures and Figs. 1 and 2.

In the crumpled phase we were not able to fit $C_R(d)$ to a simple function. This is probably due to the fact that we cannot reach very large distances in this phase. Near the transition however it is possible to fit the correlation function to a power law decay, at not too small distances. This is shown in Fig. 7. In the region $9 \leq d \leq 18$ it fits

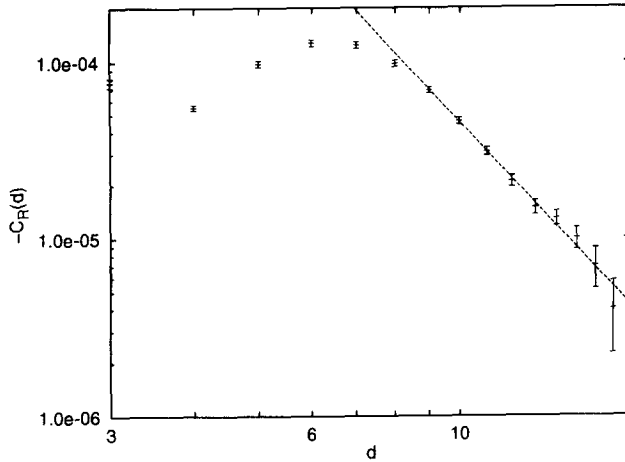


Fig. 7. Power law fit to curvature correlation $C_R(d)$ near the phase transition at $N_4 = 32\,000$ and $\kappa_2 = 1.255$.

nicely to ad^b with the result

$$a = -0.5(2) , \tag{18}$$

$$b = -4.0(2) , \tag{19}$$

$$\chi^2 = 5 \text{ at } 8 \text{ d.o.f.} \tag{20}$$

This data was made at a volume of 32 000 simplices, with $\kappa_2 = 1.255$. We used 65 configurations, which were recorded every 5000 sweeps. A similar fit using C_V gives a compatible power,

$$a = -5.7(1.6) \times 10^2 , \tag{21}$$

$$b = -4.30(12) , \tag{22}$$

$$\chi^2 = 2.3 \text{ at } 8 \text{ d.o.f.} \tag{23}$$

This result should be taken with caution, however. One would really like to have a good fit over a larger range. To get some idea of the typical ranges involved, we consider the number of triangles at a given distance d ,

$$\langle N'(d) \rangle = \left\langle \frac{\sum_{x,y} \delta_{d(x,y),d}}{N_2} \right\rangle , \tag{24}$$

where N_2 is the number of triangles of the configuration. The corresponding quantity with “triangles” replaced by “four-simplices” was studied more closely in [7]. The value d_m where $N'(d)$ has its maximum, is an indication of the distance at which finite size effects might become important. At $\kappa_2 = 1.255$, this d_m is only 11, indicating that finite size effects may play a role in the measured power.

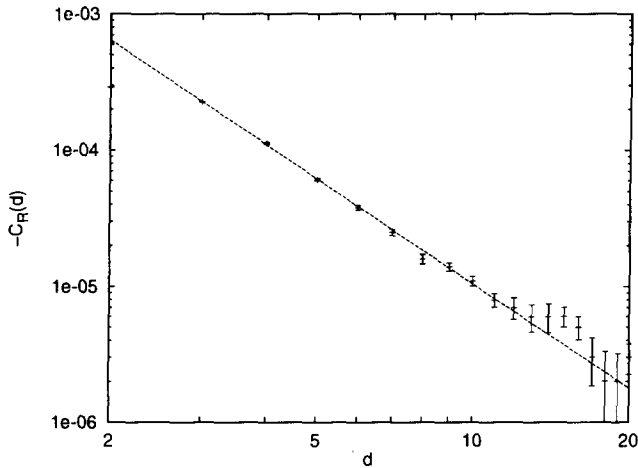


Fig. 8. Power law fit to curvature correlation $C_R(d)$ in the elongated phase at $\kappa_2 = 1.5$.

The situation is even better far in the elongated phase. Here a power law fits well, as can be seen in Fig. 8. This fit was done to the points $3 \leq d \leq 15$ and the parameters of this fit are for C_R

$$a = -0.0038(1), \quad (25)$$

$$b = -2.56(3), \quad (26)$$

$$\chi^2 = 17 \text{ at } 11 \text{ d.o.f.} \quad (27)$$

and for C_V

$$a = -2.2(1), \quad (28)$$

$$b = -2.57(2), \quad (29)$$

$$\chi^2 = 14 \text{ at } 11 \text{ d.o.f.} \quad (30)$$

The value of d with maximum number of triangles was 32, so in this case we are in a region of small distances compared to the system size. This data was made from 23 configurations of 32 000 simplices. We have also fitted the connected correlation functions at other points far in the elongated phase and at 16 000 simplices. The power that emerged was within the errors equal to the one given above.

5. Discussion

We have investigated the behaviour of the curvature and volume correlation functions. It turned out that the naive correlation functions could be almost entirely described by a “disconnected part”, which we therefore subtracted. The difference turns out to behave

according to a power law in the elongated phase and near the transition. This indicates the presence of massless excitations.

An obvious question is what the continuum observables are corresponding to the correlation functions we have measured. Generally, in a scaling region, a lattice operator is equivalent to a combination of various continuum operators, weighted with powers of the lattice distance a according to their dimensions. In a previous paper [7] we found evidence for scaling in a surprisingly wide region around the transition value of κ_2 . Assuming that the theory can be described by a continuum metric tensor $g_{\mu\nu}$ with corresponding curvature R , the continuum observable with lowest dimension corresponding to our lattice correlation function would be given by

$$C_R, C_V \rightarrow \frac{\langle \int dx \sqrt{g(x)} \int dy \sqrt{g(y)} \delta(d(x, y) - d) R(x) R(y) \rangle}{\langle \int dx \sqrt{g(x)} \int dy \sqrt{g(y)} \delta(d(x, y) - d) \rangle} - \left(\frac{\langle \int dx \sqrt{g(x)} \int dy \sqrt{g(y)} \delta(d(x, y) - d) R(x) \rangle}{\langle \int dx \sqrt{g(x)} \int dy \sqrt{g(y)} \delta(d(x, y) - d) \rangle} \right)^2, \tag{31}$$

where $d(x, y)$ is the geodesic distance between the points x and y for a given metric $g_{\mu\nu}$. The uniqueness of the lowest dimension correlation function in the continuum is in accordance with the fact that we found identical behaviour for C_R and C_V , up to an overall factor. Of course, we do not know the effective action specifying the average in (31). It could be a combination of $\int dx \sqrt{g} R$ and higher order R^2 terms.

The fact that the connected correlation function is negative suggests that it registers fluctuations in the conformal mode of $g_{\mu\nu}$.

In a previous paper [7] we explored the possibility of a semiclassical region near the transition, in which the system behaves like a four-sphere for not too small or large distances. To this end, we defined a scale dependent effective curvature. For κ_2 near the transition the following picture emerged. At small distances, this effective curvature is large, indicating a Planckian regime. At intermediate distances there seems to be a semiclassical regime, where the space behaves like a four-sphere. The fluctuations around this approximate S^4 might then correspond to gravitons. We consider it therefore encouraging that we find the power law behaviour.

For the volumes in current use, the effective curvature shows that the semiclassical regime sets in at a distance roughly 0.6 of r_m (cf. Fig. 13 in [7]). Here, r_m is the geodesic distance through the simplices where the number of simplices $N'(r)$ has its maximum. We conjectured this fraction to go down at larger volumes. Similarly, a little beyond 0.6 of $d_m = 11$ turns out to be the distance where the curvature correlations start to behave like d^{-4} in Fig. 7. We like to think of this as a confirmation of the point of view sketched above.

Two-point functions of curvature and volume have been studied in the Regge calculus formulation of simplicial quantum gravity in Refs. [9,10]. In these studies there are only results in what is called the well-defined phase of the Regge calculus approach, which corresponds to our crumpled phase. This makes it hard to do more than the qualitative comparison which was done in Section 3.

The curvature correlations have also been investigated in the continuum. In Ref. [11] they were found to be of zero range in the tree approximation to Einstein gravity. To one loop order we may expect on dimensional grounds a behaviour $G^2 d^{-8}$ in flat space, and $G^2 \bar{R}^2 d^{-4}$ for S^4 , where G is Newton's constant and \bar{R} is the S^4 background curvature.

In [12] a theory is developed for the conformal factor in four-dimensional quantum gravity and from this the curvature correlation is calculated. The conformally invariant phase discussed in [12] seems to correspond to the elongated phase in the dynamical triangulation model. Intuitively, this can be understood by visualizing large fluctuations in the conformal factor as generating many baby universes. Many baby universes is also a feature of the branched polymer like elongated phase of simplicial quantum gravity [13]. Furthermore, the conformally invariant phase would occur at very large distance scales. In [7] we argued that the elongated phase also describes scales which are large compared to a typical physical curvature scale. In this conformally invariant phase a power law is predicted for the curvature correlations (see also [14]). Unfortunately, a direct comparison with [12,14] is not possible because in the continuum the correlation function is defined as a function of the distance in a fixed fiducial metric, a quantity that is not yet defined in our model. Our result ≈ 2.6 for the power in the elongated phase is quite different from the ≈ 0.7 , which corresponds to the analogue central charge $Q^2 \approx 8$ suggested in [14].

Acknowledgements

The authors would like to thank Emil Mottola for discussions. We furthermore thank Piotr Białas for useful comments on a first version of this paper. This work is supported in part by the Stichting voor Fundamenteel Onderzoek der Materie (FOM). Most of the numerical simulations were carried out on the IBM SP1 at SARA.

References

- [1] J. Ambjørn and J. Jurkiewicz, Phys. Lett. B 278 (1992) 42.
- [2] M.E. Agishtein and A.A. Migdal, Mod. Phys. Lett. A 7 (1992) 1039.
- [3] D. Weingarten, Nucl. Phys. B 210 [FS6] (1982) 229.
- [4] M.E. Agishtein and A.A. Migdal, Nucl. Phys. B 385 (1992) 395.
- [5] J. Ambjørn, J. Jurkiewicz and C.F. Kristjansen, Nucl. Phys. B 393 (1993) 601.
- [6] S. Catterall, J. Kogut and R. Renken, Phys. Lett. B 328 (1994) 277.
- [7] B.V. de Bakker and J. Smit, Nucl. Phys. B 439 (1995) 239.
- [8] H.W. Hamber, *in* Critical phenomena, random systems, gauge theories, ed. K. Osterwalder and R. Stora (North-Holland, Amsterdam, 1986) p. 375.
- [9] H.W. Hamber, Phys. Rev. D 50 (1994) 3932.
- [10] W. Beirl, H. Markum and J. Riedler, Nucl. Phys. B (Proc. Suppl.) 34 (1994) 736.
- [11] G. Modanese, Phys. Lett. B 288 (1992) 69; Riv. Nuovo Cimento 17 (1994) 1.
- [12] I. Antoniadis and E. Mottola, Phys. Rev. D 45 (1992) 2013.
- [13] J. Ambjørn, S. Jain, J. Jurkiewicz and C.F. Kristjansen, Phys. Lett. B 305 (1993) 208.
- [14] I. Antoniadis, P.O. Mazur and E. Mottola, Nucl. Phys. B 388 (1992) 627.